



# Bayesian Computational Sensor Networks: Small-scale Structural Health Monitoring

Wenyi Wang, Anshul Joshi, Nishith Tirpankar, Philip Erickson, Michael Cline, Palani Thangaraj, and Thomas C. Henderson

University of Utah, Salt Lake City, Utah, United States

## Abstract

The Bayesian Computational Sensor Network methodology is applied to small-scale structural health monitoring. A mobile robot, equipped with vision and ultrasound sensors, maps small-scale structures for damage (e.g., holes, cracks) by localizing itself and the damage in the map. The combination of vision and ultrasound reduces the uncertainty in damage localization. The data storage and analysis takes place exploiting cloud computing mechanisms, and there is also an off-line computational model calibration component which returns information to the robot concerning updated on-board models as well as proposed sampling points. The approach is validated in a set of physical experiments.

*Keywords:* Bayesian Computational Sensor Networks, Uncertainty, Structural Health Monitoring, Cloud Computing

## 1 Introduction

Structural health monitoring of aircraft poses a significant problem in their exploitation and maintenance. To address this issue, the major specific objectives of our work are to:

1. Exploit Bayesian Computational Sensor Networks (BCSN) [14] to detect and identify structural damage. Here we demonstrate the combination of a Simultaneous Localization and Mapping (SLAM) method with the use of ultrasound to map damage in a small-scale structure.
2. Exploit an active feedback methodology using model-based sampling advice which informs the sample point selection during path planning for the monitoring task.
3. Provide a rigorous model-based systematic treatment of the uncertainty in the process, including stochastic uncertainties of system states, unknown model parameters, dynamic parameters of sensor nodes, and material damage assessments.
4. Achieve goals 1-3 exploiting cloud computing.

This work addresses 3 of the 4 DDDAS (Dynamic Data-Driven Analysis Systems) interdisciplinary research components: applications modeling, advances in mathematics and statistical algorithms, and application measurement systems and methods, and more specifically addresses several questions raised in the DDDAS-InfoSymbiotics 2010 Report [8] by Working Group 3 (WG3) Large and Heterogeneous Data from Distributed Measurement & Control Systems (Alok Chaturvedi, Adrian Sandhu): “DDDAS inherently involves large amounts of data that

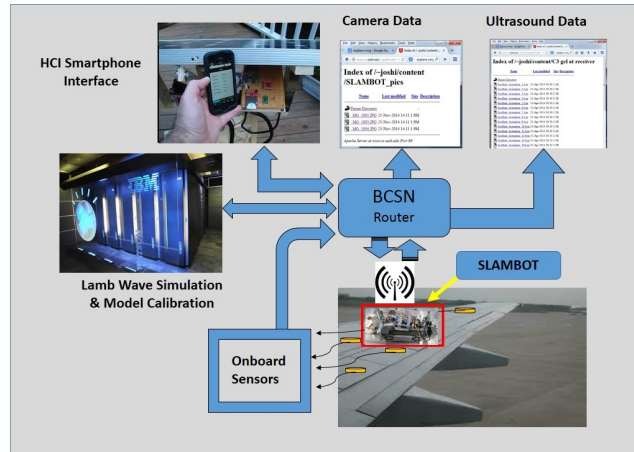


Figure 1: Small-scale Structural Health Monitoring in the Cloud.

can result from heterogeneous and distributed sources which require analysis before automatically integrating them to the executing applications that need to use the data.” Figure 1 shows a conceptual layout of the problem addressed here.

The mobile robot (SLAMBOT) is placed on the structure to be monitored (here an aircraft wing), and performs its analysis by interacting with storage and computational agents in the cloud. In our work, the interaction is mediated by means of a highly customizable data sharing model which provides low latency between sensing and computational resources (using optimized socket applications), and dynamic routing. The various components include (1) the SLAMBOT, (2) storage capabilities for image and ultrasound data, (3) off-line simulation agents which can dynamically calibrate models and provide optimal sample point locations, and (4) some form of HCI agent (e.g., smartphone app or data analysis center). For another view, see [4].

In the remainder of the paper, we describe the following aspects of the small-scale structural health monitoring system:

1. **Robot Monitoring Agents:** a high-level monitoring agent is developed using the Contract Net approach; this agent is invoked by the human inspector. It in turn contracts with the SLAMBOT to gather damage location information in terms of a map created during the ultrasound examination of the small-scale structure.
2. **Ultrasound Analysis Model:** An ultrasound range sensor is described which exploits a computational model of Lamb wave propagation through the structure to be monitored.
3. **Cloud Computing Architecture:** the cloud computing architecture allows various agents to efficiently exchange data and information.
4. **Validation Experiment:** a physical experiment using an aluminum plate, and a mobile robot is described which provides bounds on the uncertainty of the operation of the monitoring process.

## 2 Robot Monitoring Agents

The monitoring task is divided between a virtual agent which manages the monitoring process (the *manager*), and a set of inspection agents (the *contractors*) which are physical robots capable of mapping damage in the structure of interest. In addition, the *manager* may request bids on other aspects of the problem (e.g., computational simulations for model calibration, etc.). This approach has been chosen so as to make the solution more general and applicable to a wide variety of scenarios. For example, in aircraft inspection, we envision a set of SLAMBOT type robots which may be tracked ground vehicles, or quadrotors that are available to provide inspections, but which must be contracted to perform the work. The *Contract Net* protocol [21] is used which follows the following sequence:

- The *manager* agent issues a general broadcast task announcement with an eligibility specification, a task abstract, a bid specification and an expiration time.
- The *contractor* agents bid on tasks they can handle, and provide some information about their capabilities.
- The *manager* agent then awards bids (perhaps multiple).
- The *contractor* agents then proceed with the task and may exchange information with other agents as necessary to complete the task. They also store the acquired data in the cloud so that it is available to other agents involved in the process. Once the task is completed they announce that to the *manager* and submit a final report.

### 2.1 The SLAMBOT

In the current version of the system, we have developed the SLAMBOT [26] (see Figure 2).

The SLAMBOT is equipped with a camera for SLAM, and two ultrasound sensors (front and back) for damage analysis in the structure. When taking ultrasound readings, the SLAMBOT lifts itself up on the ultrasound sensors so as to press them firmly against the material surface. The SLAMBOT is built on a *Systronix Trackbot* chassis and is a differential drive robot. The vision, motion, actuation and localization algorithms are implemented on-board by a mini-computer (*pcDuino*), which runs a version of the *Ubuntu* operating system and interfaces with the robot's hardware directly. Its wi-fi capability enables it to communicate with the cloud server and other agents as necessary. The SLAMBOT is equipped with a *Logitech C250* webcam for measurement (for locating landmarks and ensuring a collision-free motion on the surface being inspected). The ultrasound sensor carried by the robot is a *VS900-RIC Vallen Systeme* high sensitivity Acoustic Emission (AE) sensor.<sup>1</sup>

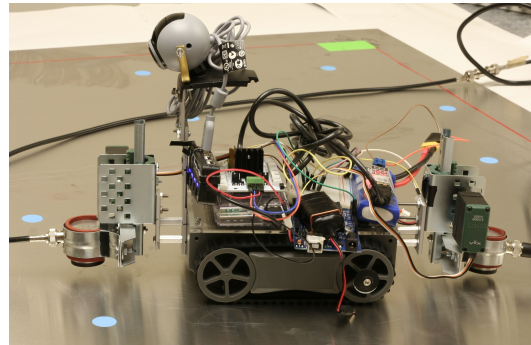


Figure 2: SLAMBOT for Structural Health Monitoring.

<sup>1</sup>From their website: "High sensitivity AE-sensor (wide band) with integral preamplifier (34 dB) and calibration bypass. Optimized for applications requiring sensitivity from 100-900 kHz. Able to drive long cables."

## 2.2 SLAM

We have implemented the SLAM algorithm from Thrun et al. [23] with the following modifications. For a landmark located at  $[x_L, y_L]^T$ , and robot pose  $[x, y, \theta]^T$ , the sensor returns the landmark's coordinates with respect to the robot frame. The return  $z = [u, v]^T$  can be written as a function of  $[x, y, \theta, x_L, y_L]^T$  as:

$$z = \begin{bmatrix} u \\ v \end{bmatrix} = h(x, y, \theta, x_L, y_L) = \begin{bmatrix} c\Delta x + s\Delta y \\ -s\Delta x + c\Delta y \end{bmatrix}$$

where  $s = \sin \theta$ ,  $c = \cos \theta$ ,  $\Delta x = x_L - x$ , and  $\Delta y = y_L - y$ .

Then the Jacobian of  $h$  at  $[x, y, \theta, x_L, y_L]^T$  is:

$$\tilde{H}(x, y, \theta, x_L, y_L) = \begin{bmatrix} -c & -s & -s\Delta x + c\Delta y & c & s \\ s & -c & -c\Delta x - s\Delta y & -s & c \end{bmatrix}$$

According to the algorithm, the sensed data is considered to be from a new landmark if the likelihood is low that it is from an existing landmark. Let  $\bar{\mu}$  be the mean of the current beliefs. The mean with new landmark locations is  $\mu = [\bar{\mu}, x_L, y_L]^T$ , where  $x_L$  and  $y_L$  are the unique values such that  $h(\bar{\mu}_x, \bar{\mu}_y, \bar{\mu}_\theta, x_L, y_L) = z$ . In our case,

$$\begin{bmatrix} x_L \\ y_L \end{bmatrix} = \begin{bmatrix} \bar{\mu}_x + \bar{c}u - \bar{s}v \\ \bar{\mu}_y + \bar{s}u + \bar{c}v \end{bmatrix}$$

where  $\bar{c} = \cos \bar{\mu}_\theta$  and  $\bar{s} = \sin \bar{\mu}_\theta$ .

The update of the covariance matrix is more complicated. Since the new landmark was unobserved before, it is natural to extend the current covariance matrix to

$$\bar{\Sigma}_{ex} = \begin{bmatrix} \bar{\Sigma} & \mathbf{0} \\ \mathbf{0} & \gamma I_2 \end{bmatrix}.$$

for some large  $\gamma$ .  $\gamma$  is taken to be in  $\Re$  to make computation possible. We use the limit result as  $\gamma \rightarrow \infty$  later in this subsection.

The Bayesian inference using the Extended Kalman Filter is given as follows. Let  $Q$  be the covariance of the sensing noise, and let  $F \in \Re^{5 \times (3+2(N+1))}$ , where  $N$  is the number of existing landmarks. All the entries of  $F$  are zeros except the upper 3 by 3 and lower 2 by 2 block matrices which are the identity. Let

$$H = \tilde{H} \begin{pmatrix} \bar{\mu}_x \\ \bar{\mu}_y \\ \bar{\mu}_\theta \\ x_L \\ y_L \end{pmatrix} F, \quad \Psi = H \bar{\Sigma}_{ex} H^T + Q, \quad K = \bar{\Sigma}_{ex} H^T \Psi^{-1}.$$

Then the new covariance is:

$$\Sigma = (I - KH) \bar{\Sigma}_{ex},$$

where in the limit case

$$\Sigma = \lim_{\gamma \rightarrow \infty} \Sigma(\gamma) = \begin{bmatrix} \bar{\Sigma} & A \\ A^T & B \end{bmatrix}$$

with  $A \in \Re^{(3+2N) \times 2}$ ,  $A_{2,i} = \sigma_{i,1} - \Delta y \sigma_{i,3}$ , and  $A_{i,2} = \sigma_{i,2} + \Delta x \sigma_{i,3}$ ;  $B \in \Re^{2 \times 2}$ ,  $B_{1,1} = c^2 q_{1,1} - 2csq_{1,2} + s^2 q_{2,2} + \sigma_{1,1} + \Delta y^2 \sigma_{3,3} - 2\Delta y \sigma_{3,1}$ , and  $B_{2,2} = s^2 q_{1,1} + 2csq_{1,2} + c^2 q_{2,2} + \sigma_{2,2} + \Delta x^2 \sigma_{3,3} + 2\Delta x \sigma_{3,2}$ , and  $B_{1,2} = B_{2,1} = c^2 q_{1,2} + csq_{1,1} - csq_{2,2} - s^2 q_{1,2} + \sigma_{1,2} + \Delta x \sigma_{1,3} - \Delta y \sigma_{2,3} - \Delta x \Delta y \sigma_{3,3}$  where  $Q = (q_{i,j})$  and  $\bar{\Sigma} = (\sigma_{i,j})$ .

### 3 Ultrasound Range Sensor

Much work has been done on the theory and application of Lamb waves to structural health monitoring (see [20, 7, 9, 10, 11, 16, 17, 27, 1, 2, 3, 5, 6, 12, 18, 19, 24, 13]). We make use of these methods in our work. Given a received signal  $f : \mathfrak{R} \rightarrow \mathfrak{R}$  and a time interval  $(t_0, t_1)$ , the range finder estimates the trivial time of maximum energy delivery that is defined by the CWT (Continuous Wavelet Transform) based scaled-average wavelet power (SAP) (see [22], p. 166 for a description of this method) in  $(t_0, t_1)$ . Define function  $peek : C^2(\mathfrak{R}) \times \mathfrak{R}^2 \rightarrow \mathfrak{R}$  such that

$$peek(f, t_0, t_1) = \arg \max_{t \in (t_0, t_1)} sap(f)(t).$$

The  $peek$  function returns a  $t$  such that the SAP of signal  $f$  is maximized in  $(t_0, t_1)$ . Then the range finder is defined by

$$\arg \max_{d \in \mathfrak{R}^+} |peek(f, t_0, t_1) - peak(sig(d), -\infty, \infty)|,$$

where  $sig(d)$  is the signal that should be received at distance  $d$  away from the actuator in the homogeneous plate. In our simulation, we model the wave propagation by the 2D Helmholtz Equation

$$\Delta u + k^2 u = g,$$

where  $g$  is the actuation signal and  $u$  is the wave function, and Sommerfeld radiation condition

$$\lim_{|\mathbf{x}| \rightarrow \infty} \sqrt{|\mathbf{x}|} (\mathbf{n} \cdot \nabla u - iku) = 0,$$

uniformly for all  $|\mathbf{n}| = 1$ . If the actuator is located at  $\mathbf{x}_s$  and emits a signal  $g$ , the solution of  $u$  is that

$$u(\mathbf{x}_r, t) = \frac{1}{2\pi} \int_{-\infty}^{\infty} d\omega \hat{g}(\omega) G(\mathbf{x}_s, \mathbf{x}_r, \omega) e^{-i\omega t},$$

$$G(\mathbf{x}, \mathbf{y}, \omega) = \frac{i}{4} H_0^{(1)}(k|\mathbf{x} - \mathbf{y}|),$$

where  $H$  is the Haenkel function, and  $k$  is the wave number that is a function of  $\omega$  in dispersive materials. For a thin plate,  $k$  can be approximated by the Lamb Wave approximation (see [25]). Our  $sig$  function is defined as

$$sig(d)(t) = u(\mathbf{x}_r, t)$$

for all  $|vx_r - vx_s| = d$ .

An ultrasound signal is transmitted by the emitter, and the receiver gets the directly propagated signal from emitter to receiver, followed by any signals reflected from features in the material (e.g., damage locations, edges, etc.). Thus, the time of arrival of the reflected signal allows the calculation of the distance traveled by that signal, and this means that the feature causing the reflection is located somewhere on an ellipse around the emitter-receiver pair.

The following discussion follows our exposition in [15]. Several measurements are needed to get the best location estimate for a feature; these range values are collected by having the robot place the actuator and receiver at different locations, and the location is constrained by the corresponding ellipse. Thus, by using an accumulator array and adding a 'vote' to each location on the ellipse, these six sensed range values allow the determination of the most likely

location of the reflecting point (damage in this case). This 'voting' is done with a Gaussian spread which leads to a smooth accumulator surface.

Observed and simulated reflected A0 mode signals with known minimized possible reflection range have significant overlap between the directly propagated and simulated reflected signals. This necessitates a method to separate reflected versus directly propagated waves in the observed data. In addition, we would like to isolate the main component of the reflected signal in the data. To achieve this, signals outside a certain reflection range are eliminated. Figure 3 shows the windowed signals versus the simulated signals as described above. In this form, the peak amplitude is not clearly identifiable. We therefore compute the CWTbased scaled-average wavelet power (SAP) (see [22] page 166, for a description of this method). The computed SAPs are shown in Figure 4; as can be seen in this figure, the peaks are more clearly discernible.

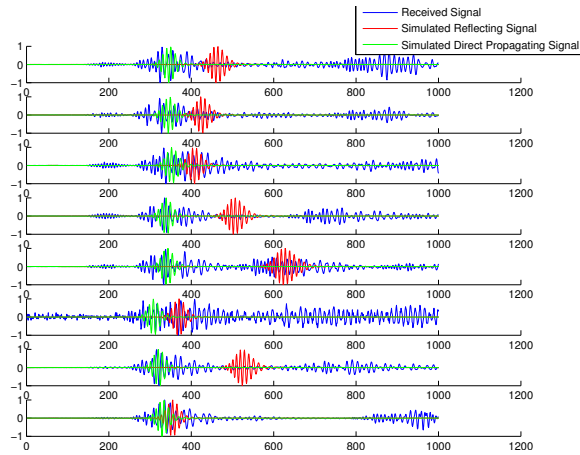


Figure 3: Windowed SAP Signal versus Simulated Signal.

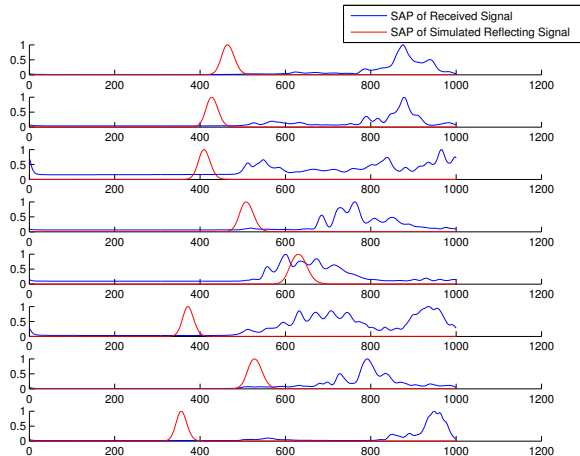


Figure 4: Computer Scaled-Average Wavelet Power (SAPs).

## 4 Data Routing Model for Distributed Cloud Computing

This is a highly customizable data sharing model between sensing and computing resources. The model enables multiple sensing nodes to open connections with computing resources and retrieve results. The presence of multiple processor and broker nodes reduces the chance of failure. RabbitMQ message broker provides reliable, flexible, highly available and multi-protocol communication system. It also provides the ability to handle multiple protocols and supports message tracing. Figure 5 shows the current implementation layout. As can be seen above, the system gains its advantages from the five main components: (1) sensor nodes, (2) router, and (3) processor nodes. A model as customizable as this enables failsafe and quick communication between resources while providing isolation between sensing and computing resources. The dynamic queuing eases development and scalability.

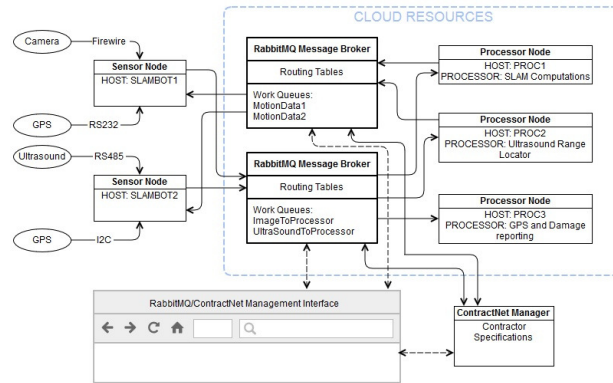


Figure 5: Cloud Component Architecture for Small-scale Health Structure Monitoring.

**Sensor Nodes** The sensors on the individual devices communicate with network connected sensor nodes which in this case are physical SLAMBots. This communication can be over the preferred sensor protocol. For example, GPS sensors can exchange data over I2C or RS-232(serial) interconnects with the nodes. The sensor nodes are applications running on host devices that have the capability of posting messages onto the rabbitMQ message broker queues. The sensor nodes gather sensor data, serialize it and put them onto the relevant work queues. Thus, they are unaware of the computing resources on the cloud. Any processor capable of handling the work posted on the relevant work queue can pick it up. Also, the node only needs to subscribe to the work queue that is relevant to it.

**RabbitMQ Message Brokers** This is a highly reliable message broker that has several built in features. This has allowed us to create a fault tolerant, persistent messaging system between processes running on disparate devices. Work queues can be spawned by remote applications dynamically. This allows creation of a highly configurable easy to use messaging system. It contains routing tables contain routing information regarding the available processing and sensing nodes.

**ContractNet Manager** This agent arbitrates allocation of work awards to sensor node agents that bid on a task. It accepts tasks provided by the user and sets up contracts. It has knowledge of contractor capabilities that it uses in making this decision.

**RabbitMQ/ContractNet Management Interface** A web interface to a service running on the message broker and contract manager allow us to monitor the messaging activity. This

helps in not only debugging the system but also in managing a large environment. This interface allows manually declaring queues, sending and receiving messages and monitor connections.

**Processor Nodes** This application runs on a remote machine that has a good computing capability. This application generally handles singular responsibilities but can also be used to consolidate data from multiple sensors and take a decision based upon the multiple data points.

## 5 Validation Experiments

The aluminum panel in the experiment is  $121.92\text{cm}^2$ , and 1.6 mm thick, the sensors were *VS900-RIC* Vallen transducers, and the excitation signal was a 200 KHz 5 cycle, Hann-windowed waveform. Figure 6 shows a trace of a sample SLAM run; as can be seen, the localization results are good for the robot and for nearby landmarks. However, more distant landmarks are poorly localized due to the failure of the underlying assumptions. We are planning on performing a multi-robot SLAM with another tracked robot on the surface and a quadrotor hovering above the plate.

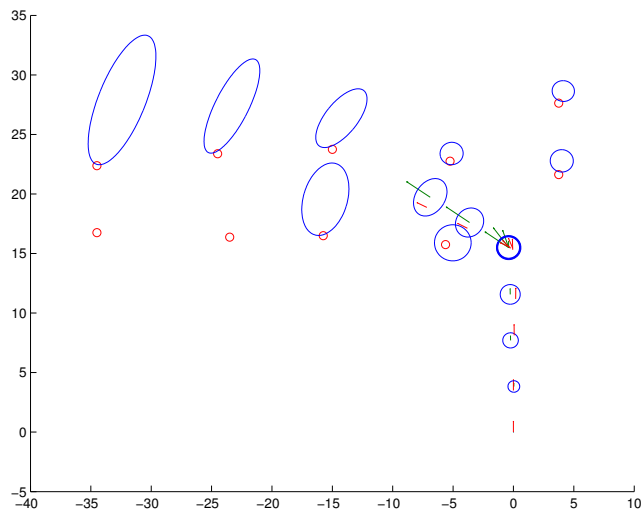


Figure 6: Results from a SLAM Run.

Figure 7 shows ellipses produced by reflections from the boundary.

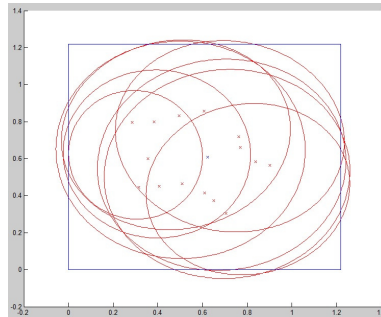


Figure 7: Range Data from the Boundary.

## 6 Conclusions and Future Work

We have developed a cloud-based architecture which supports multiple agents working together to provide a structural health monitoring capability on a small-scale structure. This includes

not only agents who contract for monitoring service and those that deliver it, but also agents that analyze the data delivered by the monitoring robot (e.g., here this includes both camera and ultrasound data; the Lamb wave based range finder function is performed by an off-line agent in Matlab and that information can be exploited by the mobile robot running Python). The combination of Lamb wave damage analysis with a robot SLAM methodology allows for more autonomous mapping of damage in structures.

We are currently investigating the following aspects of the system:

- More precise mathematical characterization of the uncertainty in the results. While the covariance matrix of the EKF SLAM method gives some insight into the uncertainty, we believe that this can be further constrained by using multiple robots, and a better understanding of the Lamb wave uncertainties.
- The system is being extended to include multiple robots in order to reduce the uncertainty in the the localization results. Moreover, we are looking to use other bases for the SLAM technique itself; e.g., Lamb wave reflection patterns at individual locations (e.g., similar to visual SLAM based on the appearance of the surface), as well as other robots to locate the ultrasound sensors on the surface.
- We also are looking at extending the system to inspecting composite materials. This will be especially important for aircraft monitoring.

**Acknowledgments** This work was supported by AFOSR-FA9550-12-1-0291. We like to acknowledge project members (John Mathews, Dan Adams, and Eddie Grant) for their input on this and related material.

## References

- [1] A.P. Albert, E. Antoniou, S.D. Leggiero, K.A. Tooman, and R.L. Veglio. A Systems Engineering Approach to Integrated Structural Health Monitoring for Aging Aircraft. Master's thesis, Air Force Institute of Technology, Ohio, March 2006.
- [2] J.P. Andrews. Lamb Wave Propagation in Varying Thermal Environments. Master's thesis, Air Force Institute of Technology, Ohio, March 2007.
- [3] M. Barker, J. Schroeder, and F. Gürbüz. Assessing Structural Health Monitoring Alternatives using a Value-Focused Thinking Model. Master's thesis, Air Force Institute of Technology, Ohio, March 2009.
- [4] B.Liu, Y. Chen, A. Hadiks, E. Blasch, A. Aved, D. Shen, and G. Chen. Information Fusion in a Cloud Computing Era: A Systems-Level Perspective. *IEEE Aerospace and Electronic Systems Magazine*, 29(10):16–24, October 2014.
- [5] M.S. Bond, J. A Rodriguez, and H.T. Nguyen. A Systems Engineering Process for an Integrated Structural Health Monitoring System. Master's thesis, Air Force Institute of Technology, Ohio, March 2007.
- [6] J.S. Crider. Damage Detection using Lamb Waves for Sructural Health Monitoring. Master's thesis, Air Force Institute of Technology, Ohio, March 2007.
- [7] Q.-T. Deng and Z.-C. Yang. Scattering of  $S_0$  Lamb Mode in Plate with Multiple Damage. *Journal of Applied Mathematical Modeling*, 35:550–562, 2011.
- [8] C.C. Douglas and A. Patra. AFOSR/NSF Workshop on Dynamic Data Driven Application systems. Unpublished report, October 2011.

- [9] V. Giurgiutiu. Tuned Lamb Wave Excitation and Detection with Piezoelectric Wafer Active Sensors for Structural Health Monitoring. *Journal of Intelligent Material Systems and Structures*, 16(4):291–305, April 2005.
- [10] S. Ha and F.-K. Chang. Optimizing a Spectral Element for Modeling PZT-induced Lamb Wave Propagation in Thin Plates. *Smart Mater. Struct.*, 19(1):1–11, 2010.
- [11] S. Ha, A. Mittal, K. Lonkar, and F.-K. Chang. Adhesive Layer Effects on Temperature-sensitive Lamb Waves Induced by Surface Mounted PZT Actuators. In *Proceedings of 7th International Workshop on Structural Health Monitoring*, pages 2221–2233, Stanford, CA, September 2009.
- [12] S.J. Han. Finite Element Analysis of Lamb Waves acting within a Thin Aluminum Plate. Master’s thesis, Air Force Institute of Technology, Ohio, September 2007.
- [13] J.B. Harley and J.M.F. Moura. Sparse Recovery of the Multimodal and Dispersive Characteristics of Lamb Waves. *Journal of Acoustic Society of America*, 133(5):2732–2745, May 2013.
- [14] T.C. Henderson. *Computational Sensor Networks*. Springer-Verlag, Berlin, Germany, 2009.
- [15] Thomas C. Henderson, Kyle Luthy, and Edward Grant. Reaction-Diffusion Computation in Wireless Sensor Networks. *Journal of Unconventional Computing*, page to appear, 2014.
- [16] B. C. Lee and W. J. Staszewski. Modelling of Lamb Waves for Damage Detection in Metallic Structures: Part I. Wave Propagation. *Smart Mater. Struct.*, 12(5):804–814, October 2003.
- [17] B. C. Lee and W. J. Staszewski. Lamb Wave Propagation Modelling for Damage Detection: I. Two-dimensional Analysis. *Smart Mater. Struct.*, 16(5):249–259, 2007.
- [18] E. Lindgren, J.C. Aldrin, K. Jata, B. Scholes, and J. Knopp. Ultrasonic Plate Waves for Fatigue Crack Detection in Multi-Layered Metallic Structures. Technical Report AFRL-RX-WP-TP-2008-4044, Air Force Research Laboratory, December 2008.
- [19] F. Ospina. An Enhanced Fuselage Ultrasound Inspection Approach for ISHM Purposes. Master’s thesis, Air Force Institute of Technology, Ohio, March 2012.
- [20] J. L. Rose. *Ultrasound Waves in Solid Media*. Cambridge University Press, Cambridge, UK, 1999.
- [21] R.G. Smith. The Contract Net Protocol: High-Level Communication and Control in a Distributed Problem Solver. *IEEE-T Computers*, C-29:1104–1113, December 1980.
- [22] Z. Su and L. Ye. *Identification of Damage using Lamb Waves*. Springer Verlag, Berlin, Germany, 2009.
- [23] S. Thrun, W. Burgard, and D. Fox. *Probabilistic Robotics*. MIT Press, Cambridge, MA, 2005.
- [24] R.T. Underwood. Damage Detection Analysis Using Lamb Waves in Restricted Geometry for Aerospace Applications. Master’s thesis, Air Force Institute of Technology, Ohio, March 2008.
- [25] W. Wang. Imaging in a Homogeneous Aluminum Plate using Ultrasonic Waves, Honors Thesis, University of Utah, December 2014.
- [26] W. Wang, T.C. Henderson, A. Joshi, and E. Grant. SLAMBOT: Structural Health Monitoring using Lamb Waves. In *Proceedings of the 2014 IEEE International Conference on Multisensor Fusion and Integration for Intelligent Systems (MFI 2014)*, Beijing, China, September 2014.
- [27] Y. Ying, Jr. J.H. Garrett, J. Harley, I.J. Oppenheim, J. Shi, and L. Soibelman. Damage Detection in Pipes under Changing Environmental Conditions using Embedded Piezoelectric Transducers and Pattern Recognition Techniques. *Jnl of Pipeline Systems Engineering and Practice*, 4:17–23, 2013.